Electronic Supplementary Material (ESI) for Journal of Materials Chemistry C.

Supplementary Information

Heteronuclear {Tb_xEu_{1-x}} furoate 1D polymers presenting luminescent properties and SMM behavior

E.Bartolomé[a], J. Bartolomé[b], A. Arauzo[b,c], J. Luzón[b,d], R. Cases[b], S. Fuertes[e], V. Sicilia[f], A. I. Sánchez-Cano[g], J. Aporta[g], S. Melnic[h], D. Prodius[h, i], S. Shova[j]

S1. EDX, PXRD and luminescence results

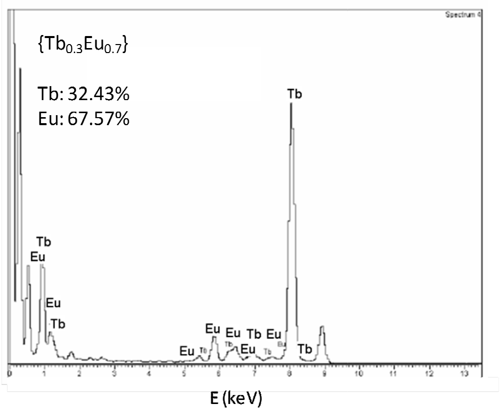

Figure S1. EDX analysis of complex {$Tb_{0.3}Eu_{0.7}$} **(4)**.

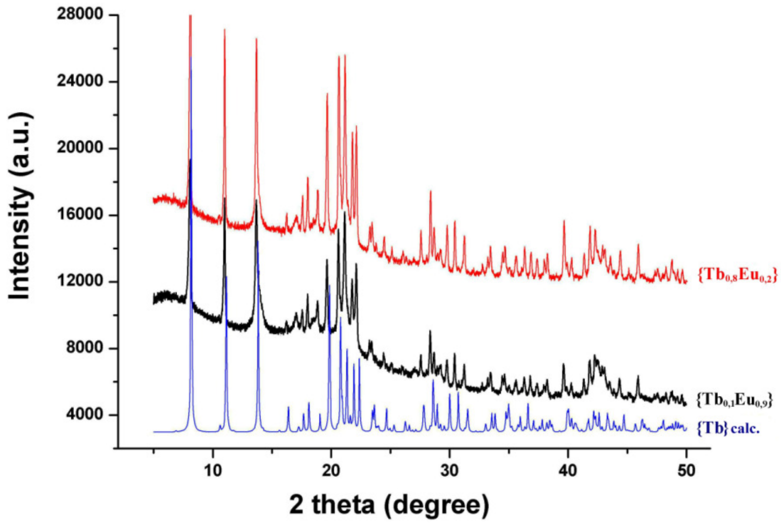

Figure S2. Comparison of calculated {Tb} (**1**) (blue) and measured X-ray powder diffraction patterns for {$Tb_{0.8}Eu_{0.2}$} (**2**) (red) and {$Tb_{0.1}Eu_{0.9}$} (**5**) (black) as representatives of isomorphous coordination polymers.

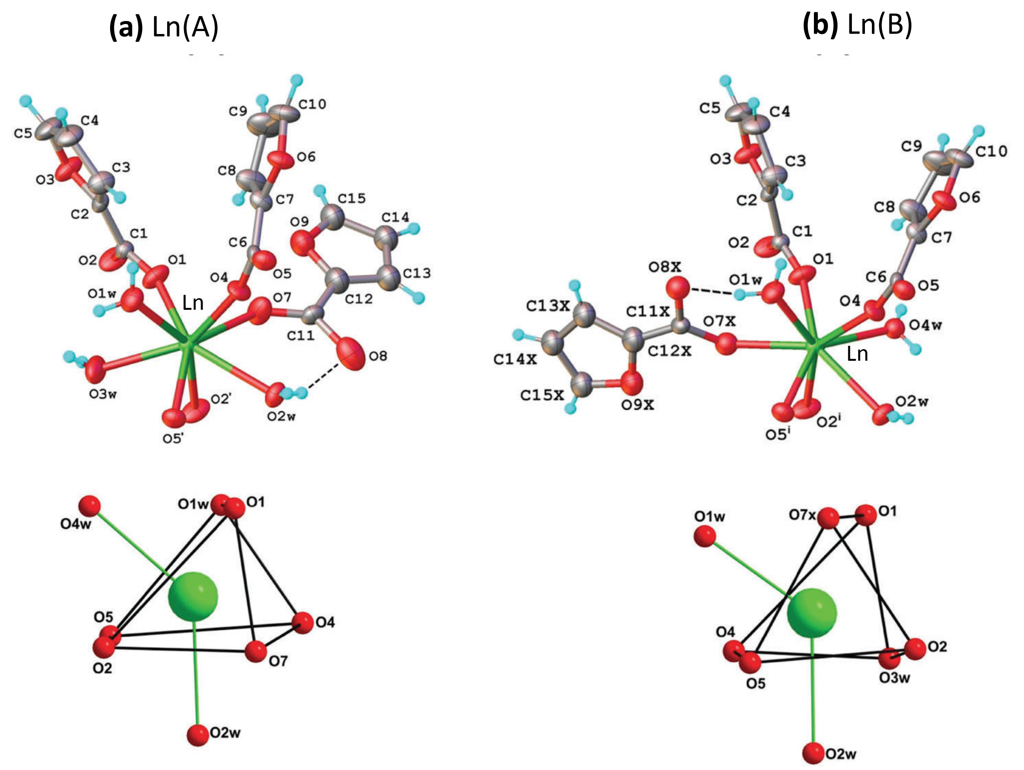

Figure S3. Two coordination environments of the Ln atom according to two positions of disordered ligands, Ln(A) and Ln(B). Thermal ellipsoids are drawn at the 50% probability level. Color code: Ln (Tb or Eu): green; O: red; C: grey, H: blue.

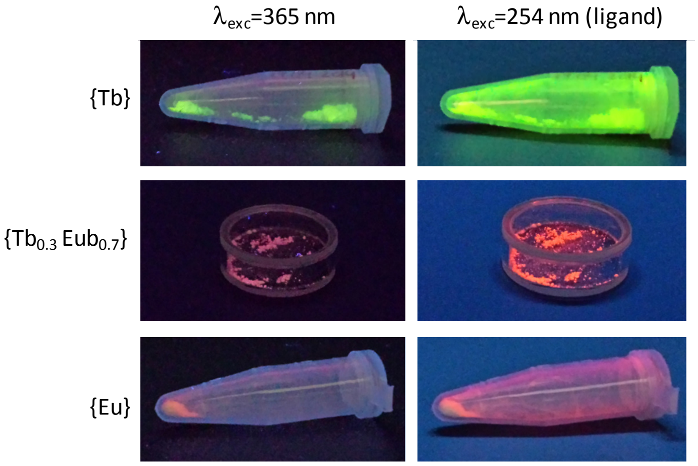

Figure S4. Photographs of the {Tb}, $\{Tb_{0.3}Eu_{0.7}\}$ and {Eu} samples under light of wavelength λ_{exc} = 365 nm (left) and λ_{exc} = 254 nm, within the absorption band of the ligand (right).

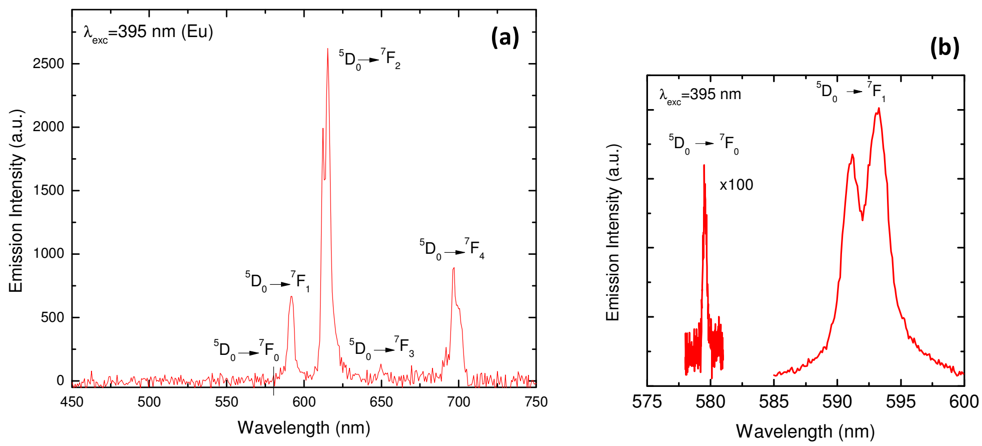

Figure S5. (a) The emission spectrum of pure {Eu} complex, excited at λ_{exc} = 395 nm of Eu (measurements performed in Hamamatsu Absolute PL QY spectrometer C11347); (b) Detail of the ${}^5D_0 \rightarrow {}^7F_0$ and ${}^5D_0 \rightarrow {}^7F_1$ peaks, measured using a higher energy resolution spectrometer equipped with a 0.5 JARREL-ASH monochromator with a Hamamatsu R928 photomultiplier tube.

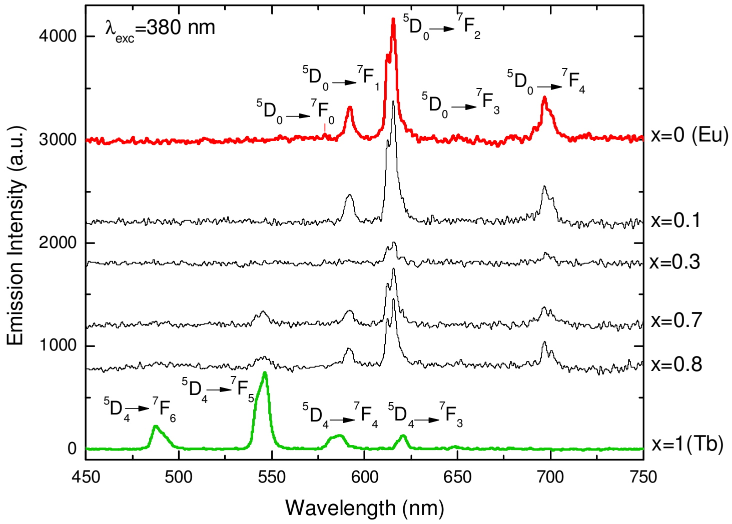

Figure S6. (a) The emission spectrum of all Tb/Eu complexes, excited at λ_{exc} = 380 nm of Tb.

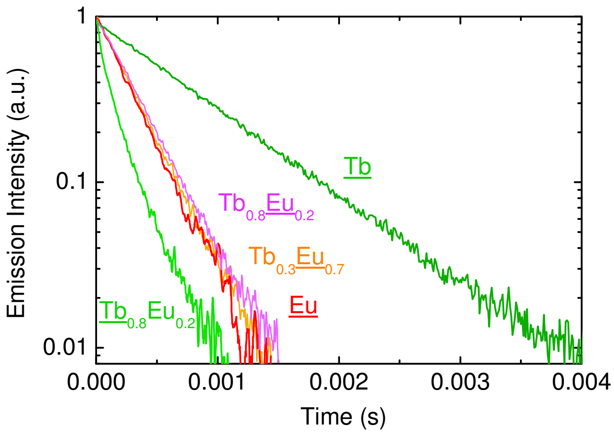

Figure S7. Emission relaxation of the {Tb} and heteronuclear complexes $\{Tb_{0.8}Eu_{0.2}\}$ and $\{Tb_{0.3}Eu_{0.7}\}$. In the case of Tb^{3+} the $^5D_4$ emitting level was excited at λ_{ex}= 487 nm, while the Eu^{3+} was excited to the $^5D_1$ level at λ_{ex}= 526 nm. The underlined ion indicates: Tb relaxation at λ_{lum}=546 nm (λ_{ex}= 487 nm), and Eu at λ_{lum}=616 nm (λ_{ex}= 526 nm).

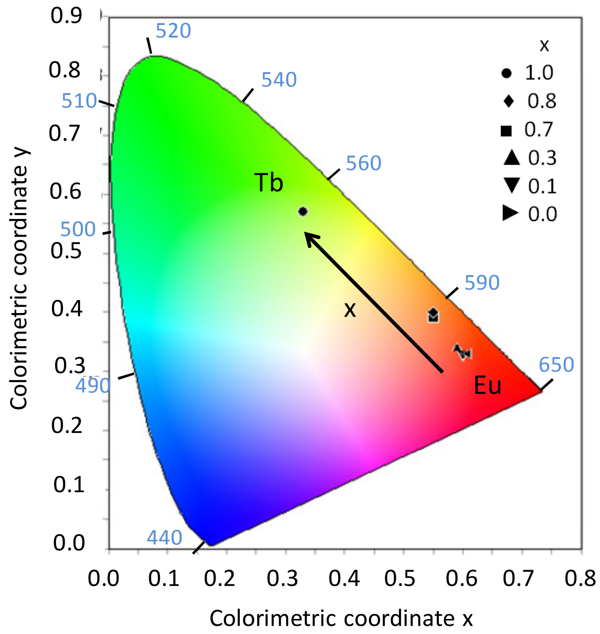

Sample	x	y
Tb	0.33	0.57
$Tb_{0.8}Eu_{0.2}$	0.55	0.39
$Tb_{0.7}Eu_{0.3}$	0.55	0.40
$Tb_{0.3}Eu_{0.7}$	0.59	0.34
$Tb_{0.1}Eu_{0.9}$	0.60	0.33
Eu	0.61	0.33

Fig. S8. Colorimetric coordinates for the {Tb_xEu_{1-x}}, x=0, 0.1, 0.3, 0.7, 0.8, 1 compounds measured under λ_{exc}=280 nm corresponding to ligand excitation.

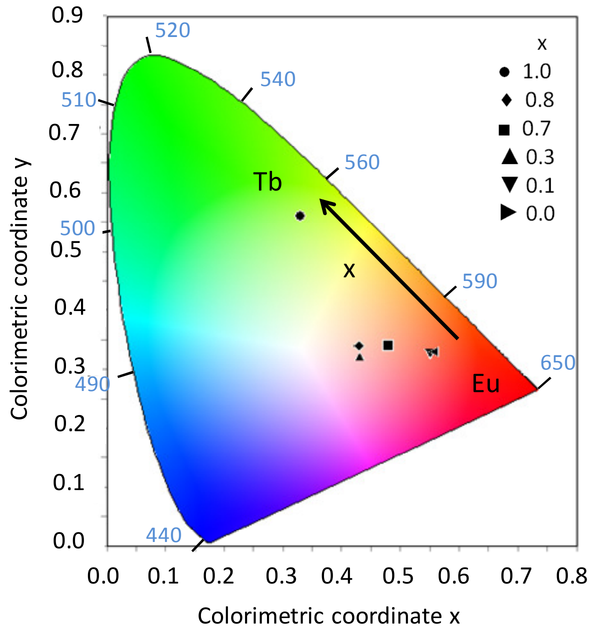

Sample	x	y
Tb	0.33	0.56
$Tb_{0.8}Eu_{0.2}$	0.48	0.34
$Tb_{0.7}Eu_{0.3}$	0.43	0.34
$Tb_{0.3}Eu_{0.7}$	0.43	0.33
$Tb_{0.1}Eu_{0.9}$	0.55	0.33
Eu	0.56	0.33

Fig. S9. Colorimetric coordinates for the {Tb_xEu_{1-x}}, x=0, 0.1, 0.3, 0.7, 0.8, 1 compounds measured under λ_{exc}=380 nm corresponding to Tb excitation.

Table S1. Luminescent properties of selected heteronuclear Tb/Eu complexes reported in the literature. Q_{Eu}^{Eu} and Q_{Tb}^{Tb} are the intrinsic quantum yields upon excitation of Eu and Tb, respectively; Q_{Tb}^{ligand} and Q_{Eu}^{ligand} are the quantum yield contributions upon ligand excitation; η_{ET} is the intermetallic Tb→Eu energy transfer.

Compound		Q_{Tb}^{ligand} (%)	Q_{Eu}^{ligand} (%)	Q_{Tb}^{Tb} (%)	Q_{Eu}^{Eu} (%)	η_{ET} (%)	Ref
$[Ln_{2-2x}Ln'_{2x}(ip)_3(H_2O)_9\cdot 6H_2O]_\infty$	Tb_2	28		32			a
	TbEu	11.1	8.3			42	
	Eu_2		10		11		
$[Ln_{2-2x}Ln'_{2x}(aip)_2(H_2O)_{10}\cdot(aip)\cdot 4H_2O]_\infty$	Tb2	32					a
	TbEu	<	0			86.8	
	Eu_2		0		8.8		
$[Ln_4(btec)_3(H_2O)_{12}\cdot 20H_2O]_\infty$	Tb_4	31.1		38.5			b
	Tb_2Eu_2	1.2	14			92	
	Eu_4		7.7		11.6		
$[Ln_{2-2x}Ln'_{2x}(bdc)_3\text{-}(H_2O)_4]_\infty$	Tb_2	45.5					c
	$Tb_{1.5}Eu_{0.5}$	0.97	13.1		19.8	90	
	TbEu	0.56	12.3		19.1	95	
	$Tb_{0.5}Eu_{1.5}$	0.19	11.9		19.1	97	
	Eu_2		13.9		16.7		
$(Tb_{1-x}Eu_x)(DPA)(HDPA)]_\infty$	$Tb_{0.95}Eu_{0.05}$					69-79	d
	$Tb_{0.5}Eu_{0.5}$					97	
$[Ln_{2-2x}Ln_{2x}'(hip)_2(H_2O)_{10},(hip),4H_2O]_\infty$	Tb_2	24		7.5			e
	TbEu	0.78		0.1	0.6	32.3	
	Eu_2				0.5		
$Tb_xEu_{1-x}(BTC).6H_2O$	Tb						f
	$Tb_{0.01}Eu_{0.99}$					48.6	
	$Tb_{0.05}Eu_{0.95}$					83.4	
	$Tb_{0.1}Eu_{0.9}$					90.9	
	$Tb_{0.4}Eu_{0.6}$					94.9	
	Eu						
$\{Tb_xEu_{1-x}(\alpha\text{-fur})_3(H_2O)_3\}_n$	**Tb**	**23.8**		**12.8**			**g**
	$Tb_{0.8}Eu_{0.2}$	**0.92**	**3.11**			**64-79**	
	Eu		**7.3**		**7.1**		

a) Freslon et al. | Inorg. Chem. 2014, 53, 1217–1228
b) Freslon et al. Inorg. Chem. 2016, 55, 794–802
c) Haquin et al. Eur. J. Inorg. Chem. **2013**, 3464–3476
d) Rodrigues et al. J. Phys. Chem. C 2012, 116, 19951–19957
e) Fan et al. J. Mater. Chem. C, 2014, 2, 5510–5525
f) Zhou et al., Inorg. Chem. Acta, 2018, 469, 576-582
g) This work.

S2. Magnetic relaxation results

Figure S10a shows ac susceptibility measurements for the mixed complex {$Tb_{0.7}Eu_{0.3}$} (**3**), at T = 2 K, H = 3 kOe. A high intensity χ'' peak is clearly observed at low frequencies, while a second bump is hinted at higher frequencies. The existence of this second relaxation process is better appreciated in the Cole-Cole plot (Fig. S10b).

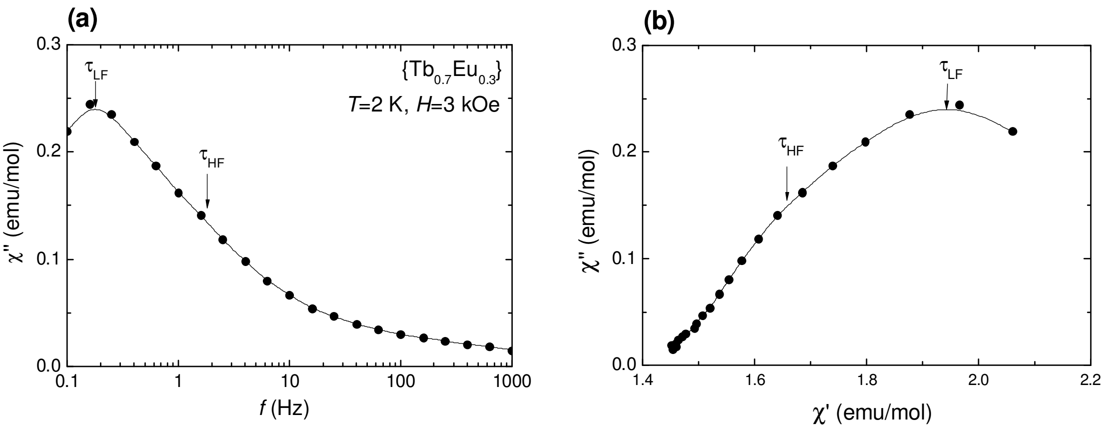

Figure S10. (a) χ''(f) measurements on mixed complex {$Tb_{0.7}Eu_{0.3}$} (**3**), at T = 2 K, H = 3 kOe; (b) Cole-Cole χ''(χ') plot, where the two relaxation processes are visible.